The Expected Performance of Gravity Probe B Electrically Suspended Gyroscopes as Differential Accelerometers

G. M. Keiser[†], Saps Buchman[†], William Bencze[†], and Daniel B. DeBra[†‡]

[†]*W. W. Hansen Experimental Physics Laboratories and*
[‡]*Department of Aeronautics and Astronautics,*
Stanford University, Stanford, CA 94303

Abstract. Four cryogenic gyroscopes on the Gravity Probe B satellite will be used to measure the precession of the local inertial reference frame with respect to a distant inertial reference frame. One of these four gyroscopes will serve as the drag-free sensor for the satellite. The other three gyroscopes, which are separated from each other by 8.25 cm, will be electrostatically supported by a digital control system. Although the gyroscopes and the electrostatic suspension system are designed to measure a precession as small as 0.1 mas/yr, any pair of these gyroscopes may also be used as a differential accelerometer. This paper analyzes the expected performance of these gyroscopes as differential accelerometers for accelerations in the frequency band from 2×10^{-3} to 2×10^{-2} Hz. The three contributions to the specific force on any one of the gyroscopes are the residual acceleration of the spacecraft, the specific forces acting between the gyroscope and the satellite, and the noise in the capacitance bridge which senses the position of the gyroscope relative to its housing. The dominant source of noise in this frequency band is found to be the quantization noise in the D/A converter used in digitally controlled electrostatic suspension system for the supported gyroscopes.

I. INTRODUCTION

The Gravity Probe B Relativity Mission (1) is a NASA supported program designed as a high precision experimental test of the General Theory of Relativity. Four gyroscopes will be used to measure two relativistic effects on gyroscopes placed in a circular, polar orbit at 650 km altitude. According to General Relativity, the geodetic or de Sitter (2) effect will cause each gyroscope to precess 6.6 arc seconds per year (as/yr) in the orbital plane, while the frame dragging, or Lense-Thirring (3), (4) effect, will cause the gyroscopes to precess 42 milliarcseconds per year (mas/yr) in a direction perpendicular to the orbital plane. The gyroscopes will be mounted in a quartz block, which is rigidly attached to a telescope. This instrument assembly will be operated at 2.3 K. During those parts of the orbit that the chosen guide star is visible, the satellite's attitude control system will keep the telescope pointed at a guide star to within 20 mas rms. In addition, the satellite will slowly roll about the line of sight to guide star at a roll rate between 0.1 and 1.0 rpm. Analysis of potential sources of error in the experiment, including the uncertainty in the proper motion of the guide star, indicates that the expected measurement accuracy will be approximately 0.2 mas/yr.

The Gravity Probe B gyroscopes are designed to measure rotations of the local inertial frame as small as 0.1 mas/year. However, these gyroscopes are also inertial sensors which may be used to measure the external forces on the spacecraft and the difference in the specific forces on the gyroscopes. One of the gyroscopes will be used as a drag-free sensor, and thrusters, which use the helium boil-off gas from the superfluid liquid helium dewar, keep gyroscope's rotor centered within its cavity. Then, the acceleration of the spacecraft itself will be a sensitive measure of the forces on the unsupported gyroscope, and the control effort of the drag free control system may be used to measure the external forces on the spacecraft (5).

M. Tapley (6), (7) carefully analyzed the use of the gyroscopes as a gravity gradiometer which could be used to measure the higher harmonics of the earth's gravitational potential. He showed that measurements of the differential specific force on two supported gyroscopes in the GP-B satellite at periods between one and ten minutes

CP456, *Laser Interferometer Space Antenna*
edited by William M. Folkner
© 1998 The American Institute of Physics 1-56396-848-7/98/$15.00

could significantly improve the knowledge of the higher harmonics of the earth's geopotential. The Gravity Probe B gyroscopes and their electrostatic suspension system are designed to minimize the torques on the gyroscopes, reliably suspend the gyroscopes, and operate compatibly with the SQUID readout system. As such, the operating conditions of the gyroscopes are significantly different from those of an accelerometer designed to reduce the specific forces on a proof mass, and they are also different from a system which is optimized to measure the gradient in the gravitational field. Nevertheless, measurements of the differential acceleration on any pair of gyroscopes will provide useful information. This paper updates Tapley's original estimates of the sensitivity of the gyroscopes as gravity gradiometers and also extends Tapley's original analysis to include several additional specific forces acting on the gyroscopes and the effects of the noise in the position readout on the noise of the gradiometer.

The following section describes the configuration of the Gravity Probe B gyroscopes in more detail. Section III is a discussion of the operation of the drag-free and electrostatic control loops. Section IV discusses physical sources of forces and force gradients acting on the gyroscopes, which determine the performance of the drag-free system. Section V summarizes the expected performance of the gyroscopes as differential accelerometers.

II. CONFIGURATION OF THE GRAVITY PROBE B GYROSCOPES

The Gravity Probe B satellite will contain four gyroscopes, three of which are electrostatically suspended and a fourth which will act the drag-free proof mass for the satellite. As shown in Figure 1, each of these four gyroscopes has three mutually perpendicular pairs of electrodes. These six electrodes are used both to sense the position of the gyroscope rotor relative to the housing and, for the supported gyroscopes, to apply a control voltage to keep the rotor centered with respect to the housing. There is also a gas spin up channel, which is used to spin the gyroscopes up to their operating speed of approximately 150 Hz. The d.c. rotor potential is determined by applying a low frequency bias which is 180^0 out of phase on opposite electrodes and by measuring the control effort required by the suspension system to prevent the rotor from moving (8). This d.c. rotor potential may be controlled by shining ultraviolet light, which enters the housing through an optical fiber, on both the rotor and the housing and using a bias electrode to control the current between the rotor and the housing (8). All surfaces on the interior of the housing are coated with a conducting coating which is electrically tied to the reference ground for the electrostatic suspension system. The radius of the rotor is 19 mm, and the gap between the rotor and the electrode is 31 μm.

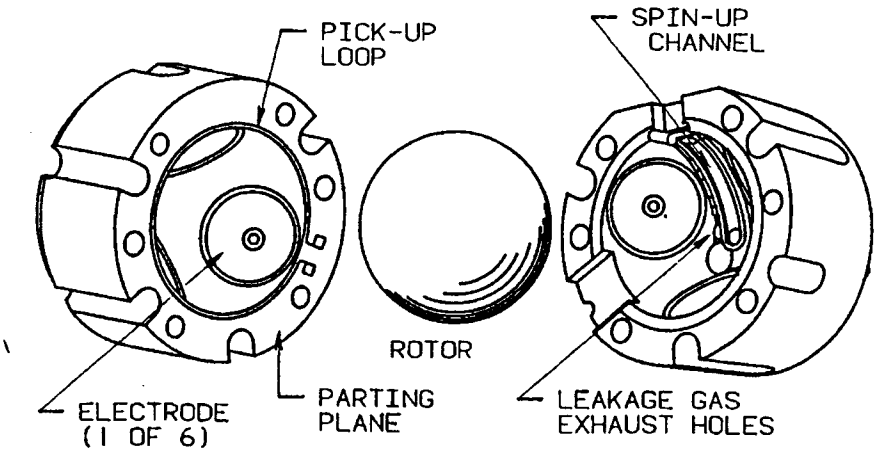

FIGURE 1. The Gravity Probe B Gyroscope

The four gyroscopes are enclosed in a fused quartz block, which is bonded to a telescope, as shown in Figure 2. The quartz block and the telescope operate within a liquid helium dewar at a temperature of 2.3 K. During those periods which the guide star is valid, the telescope remains pointed at a reference star, and the satellite rolls about the line of sight to the reference star at a fixed rate between 0.3 and 1 rpm. The rms pointing accuracy is expected to be less than 20 mas. Star sensors and rate gyroscopes external to the liquid helium dewar maintain the roll rate constant to 1 part in 10^5.

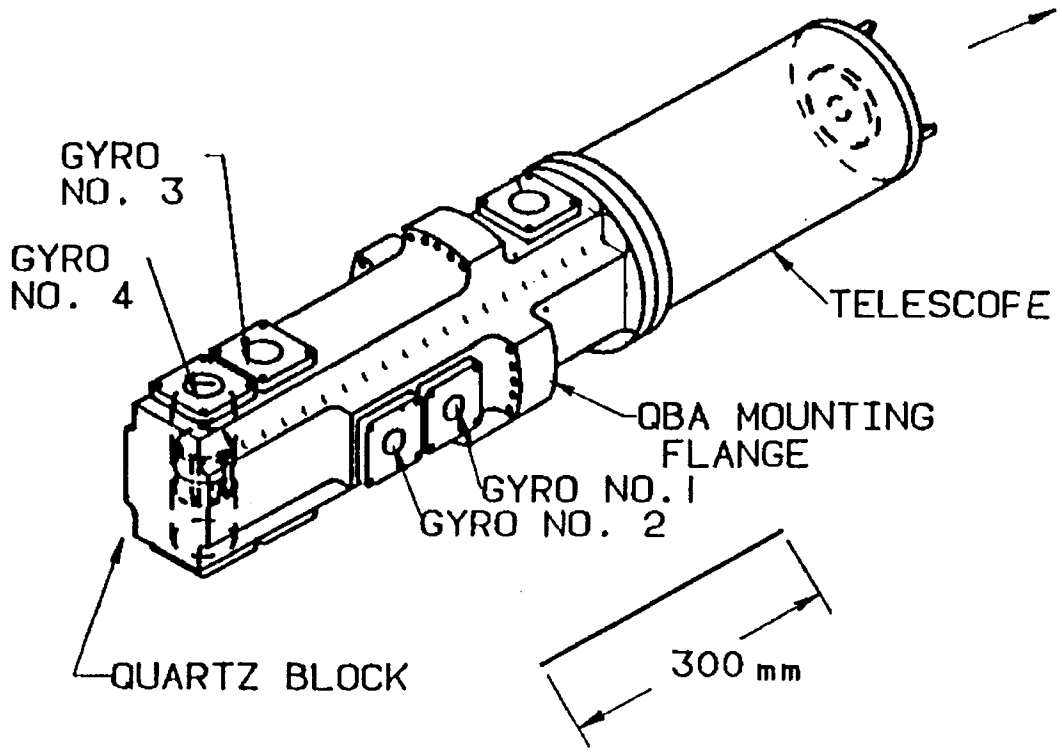

FIGURE 2. The Quartz Block Assembly. The satellite roll axis lies along the direction to the guide star.

For the unsupported gyroscope, the position of the rotor is sensed with a capacitance bridge which operates at 35 kHz and applies 40 mV peak-to-peak to the each pair of electrodes. After demodulation, the position signal is converted to a digital signal with a 16 bit A/D converter operating a 220 Hz. A digital control loop is then used to control the thrusters on the satellite so as to maintain the position of the spacecraft fixed with respect to the gyroscope rotor. For the supported gyroscopes, another digital control loop is used to vary the control voltage applied to the electrodes. The electrostatic force due to this applied voltage maintains the position of the rotor with respect to the housing.

III. EQUATIONS OF MOTION AND OPERATION OF THE DRAG FREE CONTROL SYTEM AND ELECTROSTATIC SUSPENSION SYSTEM

Under most conditions the effect of the forces due to the proof mass on the satellite may be ignored since they are considerably smaller than the other forces acting on the satellite. With this assumption, the equations of motion for the geometric center of the housing, **c**, and the center-of-mass of the rotor, **r**, are

$$M\frac{d^2\mathbf{c}}{dt^2} = \mathbf{F}_{ext} + \mathbf{F}_f$$
$$m\frac{d^2\mathbf{r}}{dt^2} + \beta\frac{d\mathbf{x}}{dt} + k\mathbf{x} = \mathbf{f} + \mathbf{f}_t \qquad (1)$$

where m and M are the masses of the gyroscope and satellite, respectively. The vector **x** is the displacement of the center-of-mass of the rotor from the geometric center of the housing, **r=c+x**. Here the geometric center of the housing is assumed to coincide with the pick-off null for the position readout system. Any d.c. offset does not change the analysis that follows, and a.c. offsets are included as noise in the position readout system. The coefficients β and k are the damping coefficient and the effective spring constant for any velocity dependent or position dependent forces acting on the rotor due to the housing. The external forces, $\mathbf{F}_{ext}$, include external forces acting on the satellite as well

as inertial forces due residual angular accelerations that are not removed by the attitude control system. The feedback forces supplied by the satellite's thrusters are denoted by $\mathbf{F}_f$. Any force acting on the gyroscope rotor including gravitational forces due to gradients in the gravitational field is represented by $\mathbf{f}$, with the exception of the feedback control force applied by the electrostatic suspension system, which is denoted $\mathbf{f}_f$. Solutions of these differential equations are discussed below for the case of the unsupported gyroscope ($\mathbf{f}_f$=0) and the supported gyroscope, where the force due to the thrusters, $\mathbf{F}_f$, is determined by the drag-free control system.

Unsupported gyroscope

For the gyroscope which acts as the drag-free sensor, there is no control force supplied by the electrostatic suspension system, $\mathbf{f}_f$=0. In this case, the feedback force on the satellite due to the helium thrusters, $\mathbf{F}_f$, supplies a force on spacecraft so that the center of the gyroscope cavity coincides with the center of the proof mass, $\mathbf{x}$=0. The dynamic solution for the equations of motion along any axis may be found by taking the Laplace transform of the equations of motion. For the drag-free control system, the Laplace transform of the feedback force is given by

$$F_f(s) = -H(s)(x(s) + n(s)) \tag{2}$$

where H(s) is the Laplace transform of the compensation network and n(s) is the Laplace transform of the position noise. These equations may be solved to find the relative position of the satellite and the drag-free gyroscope, the feedback force supplied by the drag-free control system, and the acceleration of the spacecraft and the drag-free gyroscope.

Below the bandwidth of the drag-free control system, the accelerations center of the gyroscope housing is given by:

$$s^2 c(s) \approx \frac{F_{ext}(s)}{G(s)H(s)M} + \frac{f(s)}{m} - (ms^2 + \beta s + k)\frac{n(s)}{m} \tag{3}$$

where

$$G(s) = \frac{m}{M(ms^2 + \beta s + k)}, \tag{4}$$

and the approximation has been made that the open loop gain of the servo system, G(s)H(s), is much larger than unity.

From equation (3), it can be seen that the residual acceleration of the gyroscope housing has three contributions. The first is the residual acceleration of due to external forces acting on the gyroscope and inertial forces due to angular motion of the attitude control system. The second is the contribution due to specific forces acting on the gyroscope, and the third is due to the noise in the position sensing bridge. It is interesting to note that the acceleration of the unsupported gyroscope may be considerably smaller than the acceleration of the housing. The contributions due to the residual forces and the noise in the position sensing bridge are smaller by a factor of k/ms^2 for the gyroscope than for the housing provided $k<ms^2$.

Supported gyroscope

From equation (1), the equation of motion for a supported gyroscope is

$$m\frac{d^2\mathbf{x}}{dt^2} + \beta\frac{d\mathbf{x}}{dt} + k\mathbf{x} = \mathbf{f} + \mathbf{f}_f - m\frac{d^2\mathbf{c}_s}{dt^2} \tag{5}$$

where $\mathbf{f}_f$ is the feedback force on the supported gyroscope and the other symbols have the same meaning as before. In this case, $\mathbf{c}_s$ is the position of the center of geometry of the supported gyroscope. The last term on the right hand side of this equation includes the residual acceleration of the unsupported gyroscope, given by equation (3), as well as inertial accelerations due to the angular motion of the housing of the supported gyroscope. If the feedback force is given by

$$f_f(s) = -H(s)(x(s) - n(s)), \tag{6}$$

then the closed loop expression for the feedback force may be found by substituting this expression for the feedback force into the Laplace transform of equations for motion, equation (5). Then, below the bandwidth of the servo system, the feedback force on the supported gyroscope becomes

$$f_f(s) = -f(s) - (ms^2 + \beta s + k)n(s) + ms^2 c_s(s) \tag{7}$$

This result shows that below the bandwidth of the servo system, the control effort signal has contributions from the forces acting on the unsupported gyroscope, the noise in the position sensing bridge, and the residual acceleration of the gyroscope housing.

The differential acceleration of two supported gyroscopes may be measured by comparing the control effort on two gyroscopes. In this case, the residual acceleration of the spacecraft will be a common mode signal which may be removed provided the scale factors of the control effort signal are adequately known. Tapley (7) discusses several methods of calibrating the scale factors and argues that the best method is to use the naturally occurring low degree gravity gradient of the Earth. Alternatively, the differential acceleration between one supported gyroscope and the unsupported gyroscope may be measured by monitoring the control effort signals on one of the supported gyroscopes. In this case the residual acceleration of the spacecraft may contribute to the measurement noise. In addition, small errors in the differential acceleration may occur because of differences in the closed loop gains of the drag-free control system and the electrostatic control system of the supported gyroscope. However, with this method only one control effort signal needs to be monitored.

IV. FORCES AND FORCE GRADIENTS

Electrostatic

The force on a gyroscope in the x-direction due to a potential difference between the rotor and the electrode (9) is

$$F_x = +\frac{1}{2}\frac{\partial C}{\partial x}V^2 \tag{8}$$

where C is the capacitance between the rotor and the electrode, and V is the potential difference. For two opposite electrodes along the same axis, the net electrostatic force is

$$F_{net} = \frac{1}{2}\left(\frac{\partial C_+}{\partial x}V_+^2 + \frac{\partial C_-}{\partial x}V_-^2\right) \tag{9}$$

Here, the subscripts + and – denote two opposite electrodes on the same axis. The variation in the net electrostatic force due to changes in the position, x, and the voltages, V_+ and V_-, is then

$$\begin{aligned}\delta F_{net} &= k_x\delta x + \frac{\partial F_{net}}{\partial V_+}V_+\frac{\delta V_+}{V_+} + \frac{\partial F_{net}}{\partial V_-}V_-\frac{\delta V_-}{V_-} \\ &= k_x\delta x + F_{net}\left(\frac{\delta V_+}{V_+} + \frac{\delta V_-}{V_-}\right) + \frac{1}{2}mh\left(\frac{\delta V_+}{V_+} - \frac{\delta V_-}{V_-}\right)\end{aligned} \tag{10}$$

where the negative spring constant is given by

$$k_x = \frac{\partial F_{net}}{\partial x} = \frac{1}{2}\left(\frac{\partial^2 C_+}{\partial x^2}V_+^2 + \frac{\partial^2 C_-}{\partial x^2}V_-^2\right) \tag{11}$$

and the preload acceleration, h, is given by

$$h = \frac{1}{m}\left(\frac{\partial F_{net}}{\partial V_+}V_+ - \frac{\partial F_{net}}{\partial V_-}V_-\right) \tag{12}$$

In equations (10) and (11), the assumption has been made that the electrodes are driven by a voltage source there is no substantial change in the rotor potential with a displacement of the rotor. The noise in the net applied force depends on whether the variations in the voltages, V_+ and V_- are correlated, anticorrelated, or uncorrelated. Below the bandwidth of the servo system, the net force is approximately equal to the external force.

Control Voltages

The system is normally operated so that the voltage on the positive electrode is the sum of a preload voltage, V_p, and a feedback voltage, V_f, while the voltage on the negative electrode is the the preload voltage minus the feedback voltage. The preload acceleration may then be defined as the acceleration required to drive on of the electrode voltages to zero. Under normal operating conditions, the preload acceleration is larger than the specific

acceleration on the gyroscopes, so that the preload voltage is larger than the feedback voltage. Then, the negative spring constant is approximately equal to

$$k_x = 2\frac{C_0}{d_0^2}V_p^2 \tag{13}$$

Using a value of 80 pF for the capacitance and 30 microns for the gap, the negative spring constant for a preload voltage of 0.1 volts is 1.8×10^{-3} kg/sec^2. This negative spring constant corresponds to a natural frequency of 0.027 Hz. Below this frequency, the transfer function of the gyroscope is frequency independent thereby reducing the open loop gain. The specific force noise due to the position bridge of 0.1 nm/$\sqrt{\text{Hz}}$ and this negative spring constant and is equal to 2.9×10^{-12} m/sec$^2\sqrt{\text{Hz}}$.

Since the feedback voltages applied to the two opposite electrodes are out of phase with one another and are a small fraction of the preload voltage, the noise due to the D/A converters on the two electrodes will be anticorrelated. In this case, the noise force on the rotor due to the D/A converter is given by the last term in equation (10)

$$\delta F_{net} = \frac{1}{2}mh\left(\frac{\delta V_+}{V_+} - \frac{\delta V_-}{V_-}\right) \approx mh\frac{\delta V_q}{V_p} \tag{14}$$

where the quantization noise (10) is given by

$$\delta V_q = \frac{q}{\sqrt{12 f_c}} \tag{15}$$

where q is the quantization step size and f_c is the conversion rate. For a 16 bit D/A converter operating over a range of 100 volts with a conversion rate of 220 Hz, the quantization noise is 30 μV/$\sqrt{\text{Hz}}$. If the preload accelertion is 10^{-6} m/sec^2 with a nominal operating voltage of 0.11 volts, then the specific force acting on the gyroscope is 2.6×10^{-10} m/sec$^2\sqrt{\text{Hz}}$. A considerable reduction in this noise could be achieved either by reducing the range over which the D/A converter operates or by reducing the preload acceleration. The preload acceleration is limited by the expected maximum acceleration on the supported gyroscopes, and the wide range of the D/A converter was chosen to increase the reliability of the suspension system in the event of mirco-meteoroid impacts

The thermal effects on the control voltages are likely to be correlated between the opposite electrodes since the amplifiers are expected to be in the same thermal environment. Then, from equation (10) the contribution to the change in the net force produced by the control voltages will be proportional to the net force acting on the supported gyroscopes. The electrostatic suspension system is designed to maintain the control voltages constant to better than 1 part in 10^5 at roll frequency, which is expected to be the frequency of the dominant disturbance in the frequency band from 2×10^{-3} to 2×10^{-2} Hz. Although thermal variations may produce a coherent signal at roll as large as 10^{-11} m/sec^2, the white noise is expected to be less than 10^{-13} m/sec$^2/\sqrt{\text{Hz}}$ when averaged over periods as long as 10^4 seconds.

Position Sensing and Charge Measurement Voltage

A 40 mV peak-to-peak signal at 35 kHz is applies to the same electrodes which are used to apply the control voltage. This signal produces a negative spring constant of 3.5×10^{-5} kg/sec^2 on the both the supported and the unsupported gyroscopes. For the supported gyroscopes, this negative spring constant is small compared to the negative spring constant produced by the control voltages so its contribution to the noise may be ignored. However, for the unsupported gyroscope, this position sensing voltage makes a significant contribution to the negative spring constant. The natural frequency for this negative spring constant is 3.8 mHz, which is close to the lower end of the bandwidth of interest. Then above this natural frequency, from equations (3) and (7), the contribution to the specific force due to the noise in the position sensing circuit increases as the square of the frequency. At the midpoint of the bandwidth of interest, 7×10^{-3} Hz, the specific force noise due to the noise in the position sensing bridge is 1.9×10^{-13} m/sec$^2\sqrt{\text{Hz}}$ with a bridge noise of 10^{-10} m/$\sqrt{\text{Hz}}$.

Since the position sensing voltages applied to opposite electrodes are generated from the same frequency oscillator, fluctuations in the rms voltage are likely to generate little net specific force noise. The dominant frequency component of the thermal variations is expected to be at the roll frequency, and the voltages are specified to be stable to less than 20 μV at this frequency. However, there will only be a net force on the rotor if does not lie at the force center of the housing. Assuming a constant miscentering of 4% of the gap between the rotor and the electrode, from

equation (9) the d.c. specific force on the rotor is 6.8×10^{-10} m/sec^2. The variation in this miscentering at roll frequency is expected to be less than 0.3 nm, do the variation in the force at this frequency is 5×10^{-13} m/sec^2. Averaged over periods as long as 10^4 seconds, the white noise close to this frequency is expected to be negligible.

The input current noise of the amplifier which is used to measure the output of the capacitive position sensing bridge is approximately 1 pA/$\sqrt{\text{Hz}}$. This current noise, when it is applied to the 15K impedance of the capacitance bridge at the bridge operating frequency of 35 kHz, produces a voltage noise with a spectral density of 1.5×10^{-8} volts/$\sqrt{\text{Hz}}$ near 35 kHz. Combined with the 20 mV, 35 kHz bridge excitation voltage, this amplifier current noise produces a specific force noise of 1.2×10^{-14} m/(sec$^2\sqrt{\text{Hz}}$) on the 63 g rotor.

Voltages having an amplitude of 10 mV are applied to opposite electrodes to measure the net rotor potential using the force modulation method (8). These voltages are applied at 0.05 Hz for the supported gyroscopes and 4 Hz for the unsupported gyroscope. These voltages contribute to the negative spring constant but make no additional contribution to the specific force noise due to the noise in the position bridge since the natural frequency is below the frequency band of interest.

Charged Rotor and Asymmetric Ground Plane

If the rotor becomes charged and there is an asymmetry in the ground plane of the electrodes, then the force on the rotor is

$$F_Q = \frac{1}{2}\frac{\Delta C}{d_0}\left(\frac{Q}{C}\right)^2 \tag{16}$$

Here ΔC is the asymmetry capacitance between the rotor and the ground plane, d_0 is the electrode-to-rotor gap, Q is the total charge on the rotor, and C is the total capacitance between the rotor and the housing. For an asymmetry in the capacitance of 50 pF (5% of the total capacitance), a gap of 30 microns, and a rotor potential due to the charge of 15 mV, the specific force on a 63 g rotor is 3×10^{-9} m/sec^2. This charge is expected to vary slowly with time, with typical rates of 1 mV/day. The random noise associated with this slow variation in the charge is not expected to make a significant addition contribution to the noise in the frequency band of 2×10^{-3} to 2×10^{-2} Hz.

The force between the plates of a parallel plate capacitor which has a constant charge is independent of the gap between the electrodes. In this case, the force gradient or effective spring constant is zero. However, when the asymmetry is a small fraction of the total capacitance between the electrode and the rotor, the effective spring constant becomes

$$k_x = -\frac{\partial F}{\partial x} \approx \frac{\Delta C}{d_0^2}\left(\frac{Q}{C}\right)^2 \tag{17}$$

The negative spring constant associated with the charged rotor where the rotor potential is 15 mV is 1.2×10^{-5} kg/sec^2, which gives a natural frequency of 2.2×10^{-5} Hz.

Patch or Contact Potential Effects

For variations in the rotor potential due to patch fields that are larger than the gap, the electric field is given approximately by

$$E = \frac{V_a(\theta,\phi) - V_b(\theta,\phi)}{d(\theta,\phi)} \tag{18}$$

and the total energy stored in the electric field

$$\begin{aligned} W &= \frac{\varepsilon_0}{2}\int_{volume} E^2 dV = \frac{\varepsilon_0 r_0^2}{2}\int_{solid\ angle} d\Omega \frac{\left(V_a(\theta,\phi) - V_b(\theta,\phi)\right)^2}{d(\theta,\phi)} \\ &\approx \frac{\varepsilon_0 r_0^2}{2d_0}\int_{solid\ angle} d\Omega\left(1 - \frac{\Delta d(\theta,\phi)}{d_0} + \left(\frac{\Delta d(\theta,\phi)}{d_0}\right)^2\right)\left(V_a(\theta,\phi) - V_b(\theta,\phi)\right)^2 \end{aligned} \tag{19}$$

where $\Delta d(\theta,\phi)$ is the variation in the rotor-to-housing gap and d_0 is the nominal gap. The energy stored in the electrostatic field as a function of the displacement in a direction z is given by setting

$$\Delta d(\theta,\phi) = z\cos\theta \tag{20}$$

Then, the force on the rotor in the z-direction is equal to

$$F_z = +\frac{\partial W}{\partial z}\bigg|_{V=const.} = -\frac{\varepsilon_0 r_0^2}{2d_0^2}\int_{solid\ angle} d\Omega \cos\theta\left(V_a(\theta,\phi) - V_b(\theta,\phi)\right)^2 \tag{21}$$

and the spring constant is

$$k_z = -\frac{\partial F_z}{\partial z} = -\frac{\varepsilon_0 r^2}{d_0^3}\int_{solid\ angle} d\Omega \cos^2\theta\left(V_a(\theta,\phi) - V_b(\theta,\phi)\right)^2 \tag{22}$$

The magnitudes of these quantities are strongly dependent on the size of the patches. A large number of randomly oriented patches, which are small compared to the diameter of the gyroscope rotor, will not contribute significantly to a cosine distribution of the square of the potential difference. Then, the patch effect force and force gradients should be reduced by the square root of the number of patches on the surface of the rotor. In addition, Speake (11) has shown that for parallel surfaces where the patch field is much smaller that the gap, the patch effect fields are exponentially attenuated by the ratio of the gap to patch effect field size. The grain size of the coating on the surface of the housing has been measured to be approximately 6 mircons (12) compared to a gap between the gyroscope rotor and housing of 31μm. Typical values of the patch effect potentials are 0.1 volts (11) (other ref.). Taking these two factors into account, the magnitude of the specific force acting on the gyroscope is approximately 7 $\times$ 10^{-14} m/sec^2, and the force gradient is 1 $\times$ 10^{-10} kg/sec^2, which corresponds to a natural frequency of 3 $\times$ 10^{-6} Hz with a 63 g gyroscope rotor.

The spin and polhode motion of the gyroscope and the roll of the satellite will modulate the force and force gradient on the gyroscope rotor. Since the force and force gradient depend on the square of the difference in rotor potential, patch effect forces and force gradients on the rotor could exist if the housing potential is nonuniform even though the potential on the surface of the rotor was perfectly uniform. In this case, the patch effect forces and force gradients would be constant in a housing-fixed reference frame. A nonuniform potential on the spinning rotor's surface could still produce an average d.c. force. However, this force would be modulated at the polhode period because the orientation of the spin axis in the rotor changes at the polhode period. From the expressions for the force and force gradients, it can be seen that the force and force gradients also depend on the cross correlation between the rotor and housing potentials. Since the rotor spin axis is always aligned with the satellite roll axis to within 100 arc seconds, there should be very little modulation of this cross-correlation at the satellite roll frequency. Since the spin-averaged rotor potential is modulated at the satellite roll frequency, the cross correlation in the rotor to housing potential should also be modulated at this frequency.

Gravitational

The gradient in the gravitational field of the spherical earth will produce an acceleration of each of the three supported gyroscopes. For a gyroscope separated by 25 cm from the unsupported gyroscope, value of this acceleration at a 650 km altitude orbit averaged over the orbital period is 1.4 $\times$ 10^{-7} m/sec^2. In addition, there is a component of this acceleration which has a magnitude of 4.3 $\times$ 10^{-7} m/sec^2 and rotates in the orbital plane at twice the orbital rate. The gravitational acceleration due to the J2 term in the expansion of the earth's gravitational potential will cause a differential acceleration of the gyroscopes which is approximately 1000 times smaller(13).These accelerations are extremely well known and may be used to calibrate the readout any pair of the gyroscopes which are used as differential accelerometers.

The gravitational force of the satellite on the unsupported gyroscope will accelerate the satellite in direction body-fixed direction. Because the satellite rolls about the line of sight to the guide star, the roll-averaged acceleration will lie along the direction of the satellite's roll axis. Although this acceleration will slightly modify the orbit, it will have a negligible effect on the gyroscope drift rate or the performance of the gyroscopes as differential accelerometers. A careful analysis of the mass distribution on the satellite (14) has estimated this acceleration to be as large as 5 $\times$ 10^{-8} m/sec^2. The differential specific force on the gyroscopes due to the gravitational attraction of the satellite has also been estimated to be less than 1.5 $\times$ 10^{-8} m/sec^2 and varies from gyroscope to gyroscope. The gravitational force gradient is estimated to be 5.7 $\times$ 10^{-9} kg/sec^2. This force gradient is small compared to the force gradients due to the electrostatic forces and is expected to make no significant change in the effective spring constant.

The differential gravitational acceleration due to mass motion of the satellite will produce noise in the acceleration measurements. The three independent measurements will allow an estimation of the magnitude of this

effect. The variation in the gravitational acceleration due to motion of the superfluid liquid helium will be reduced because of the centrifugal forces on the liquid helium and because of baffles installed within the liquid helium dewar. The differential gravitational acceleration due to the thermal motion of the solar panels has been estimated to be less than 5.7×10^{-13} m/sec^2. In addition, only a small fraction of this gravitational acceleration noise will lie in the frequency band of interest.

Inertial

Transforming from an inertial reference frame to a rotating reference frame, the acceleration of the center of the gyroscope housing is given by

$$\left.\frac{d^2\mathbf{c}_s}{dt^2}\right|_{inertial\ frame} = \left.\frac{d^2\mathbf{c}_s}{dt^2}\right|_{rotating\ frame} + \frac{d\boldsymbol{\omega}}{dt}\times\mathbf{d} + 2\boldsymbol{\omega}\times\mathbf{v} + \boldsymbol{\omega}\times\boldsymbol{\omega}\times\mathbf{d} \qquad (23)$$

where **d** is the displacement of the supported gyroscope from the unsupported gyroscope. The first term on the right hand side of this equation is the acceleration in the rotating frame; the second term is the tangential rotational acceleration (6); the third term is the Coriolis acceleration; and the fourth term is the centrifugal acceleration. These inertial forces acting on the unsupported gyroscopes have been thoroughly investigated by M. Tapley (6) and are only briefly summarized here.

Centrifugal Acceleration

The magnitude of centrifugal acceleration acting on the gyroscopes due to the rotation of the satellite is given by

$$a_{cf} = \omega^2 d_p \qquad (24)$$

where d_p is a small displacement of the center of mass of the gyroscope from the satellite's axis of rotation and ω is the angular rotation rate. The drag free control system will cause the satellite to rotate about the center of geometry of the unsupported gyroscope. For a displacement of the center of mass of any of the supported gyroscopes from the center of geometry of the supported gyroscope as large as 0.01 cm (4 milli-inches) and an angular rotation rate of the satellite of 1 rpm, the centrifugal acceleration is 10^{-6} m/sec^2. The force necessary to counteract this acceleration is expected to be one of the dominant forces acting on the supported gyroscopes. The satellite roll rate is expected to be stable to 1 part in 10^5 at roll frequency, which will produce a variation in the centrifugal acceleration of 2×10^{-11} m/sec^2 at roll frequency. The random noise close to roll frequency is not expected to be a significant contributor to the overall random noise.

The specific force gradient due to the satellite's roll rate is then simply equal to the square of the angular rotation rate. For a rotation rate of 1 rpm, the specific force gradient is 0.01 /sec^2, which corresponds to an effective negative spring constant of 6.3×10^{-4} kg/sec^2 and a natural frequency of 0.017 Hz. For a displacement noise of 0.1 nm/$\sqrt{\text{Hz}}$, the additive readout noise is 10^{-12} m/sec$^2\sqrt{\text{Hz}}$. This negative spring constant only applies to those directions perpendicular to the satellite roll axis for the supported gyroscopes.

Tangential Rotational Acceleration due to Pointing Control System

The next term on the right hand side of equation (23) produces noise due to the pointing control system in a direction perpendicular to the satellite roll axis. The rms noise of the pointing control system is expected to be on the order of 20 mas. However, the tangential rotational acceleration (6) due to this term in the equation of motion, produces noise which is proportional to the angular acceleration. If the noise in the pointing control system is white, then the angular acceleration increases as the square of the frequency up to the bandwidth of the pointing control system. A simulation of the pointing control system (15) shows a coherent pointing error at roll frequency of approximately 2 mas and a random noise close to this frequency of approximately 10 mas/$\sqrt{\text{Hz}}$, which is dominated by the noise in the telescope readout. For a gyroscope separated from the drag free gyroscope by 8.25 cm, the tangential rotational noise is 2.5×10^{-12} m/sec^2 at a roll frequency of 1 rpm with a random noise component of 1.25×10^{-11} m/sec$^2\sqrt{\text{Hz}}$ close to roll frequency.

TABLE 1. Dominant Sources of Specific Force due to Noise in Position Sensing Bridge

	Spring Constant kg/sec^2		Natural Frequency Hz		Specific Force Noise m/(sec$^2\sqrt{Hz}$)	
Source	Supported	Unsupported	Supported	Unsupported	Supported	Unsupported
Control Voltages	1.8×10^{-3}	-	0.027	-	2.9×10^{-12}	-
Position Sensing Voltage	3.5×10^{-5}	3.5×10^{-5}	0.0038	0.0038	no additional	1.9×10^{-13}
Charge Measurement	9.7×10^{-6}	9.7×10^{-6}	0.0019	0.0019	no additional	no additional
Patch Effect	1×10^{-10}	1×10^{-10}	3×10^{-6}	3×10^{-6}	no additional	no additional
Centrifugal Acceleration ⊥	6.3×10^{-4}	-	0.01	-	1.0×10^{-12}	-

⊥ Perpendicular to the direction of the satellite roll axis

Other Forces Acting on Gyroscopes

Because of the unique environment of the Gravity Probe B gyroscopes other forces acting on the gyroscope are not expected to contribute significantly to the forces or force gradients acting on the gyroscopes. Thermal radiation pressure forces are reduced because of the 2.3 K operating temperature, and the radiometer effects are expected to be negligible because of the operating pressure of less than 10^{-11} Torr. Similarly, damping of the gyroscope motion the residual gas within the gyroscope housing is expected to be small compared with the forces applied by suspension system. The gyroscopes operate within a superconducting magnetic shield where the residual magnetic field is less than 3×10^{-6} gauss, and external magnetic fields are attenuated by twelve orders of magnitude. Because of this environment forces and force gradients due to magnetic forces are expected to be negligible.
Cosmic Rays?

V. EXPECTED SYSTEM PERFORMANCE

The difference in the specific force acting on the gyroscopes is the sum of the contribution from the noise in the position sensing bridge and the contribution from the specific force noise acting on the gyroscopes. Contributions from the noise in the position sensing bridge are proportional to $(ms^2+\beta s+k)n(s)$, so that the specific force at any given frequency depends on the values of the mass, the negative spring constant, and the noise in the position sensing bridge. The table below summarizes the dominant contributions to the specific force noise due to the noise in the position sensing bridge in the frequency band from 2×10^{-3} Hz to 2×10^{-2} Hz.

The contributions to the specific force from various sources are shown in Table 2 below. Estimates are given for both the maximum d.c. force and the spectral density of the specific force acting both the supported and unsupported gyroscopes. Noise in the pointing control system introduces a large specific force noise in the direction perpendicular to the separation between the gyroscopes.

TABLE 2. Dominant Sources of Specific Force Acting on the Gyroscope

	Maximum D.C. Specific Force (m/sec^2)		Spectral Density of Specific Force at 7×10^{-3} Hz (m/sec$^2\sqrt{Hz}$)	
Source	Supported	Unsupported	Supported	Unsupported
A/D Converter on Control Voltages	-	-	2.6×10^{-10}	-
Thermal Stability of Control Voltages	10^{-11} (roll)	-	$< 10^{-13}$	-
Miscentering and Position Sensing Voltage	6.8×10^{-10}	6.8×10^{-10}	-	-
Back-Reaction of Position Sensing Circuit	-	-	1.2×10^{-14}	1.2×10^{-14}
Charge Rotor and Asymmetric Ground Plane	$< 3 \times 10^{-9}$	$< 3 \times 10^{-9}$	-	-
Patch Effect forces	7×10^{-14}	7×10^{-14}	-	-
Gradient in Earth's Gravitational Field	$<5.6 \times 10^{-7}$	-	-	-
Centrifugal Specific Force ⊥	$< 1 \times 10^{-6}$	-	-	-
Tangential Rotation Acceleration ⊥	2.5×10^{-12}	-	1.25×10^{-11}	-

⊥ Perpendicular to the direction of the satellite roll axis only

These results indicate that the Gravity Probe B gyroscopes may be used as differential accelerometers and are expected to have an overall accuracy of 2.6×10^{-10} m/(sec$^2\sqrt{\text{Hz}}$) in the frequency range from 2×10^{-3} to 2×10^{-2} Hz. The dominant source of noise is the quantization noise in the D/A converter for the control voltages on the supported gyroscopes. The design of the gyroscopes and the electrostatic suspension system have not been optimized to improve the performance as differential accelerometers but, instead, have been optimized to reduce the torques acting on the gyroscopes, provide reliable suspension of the spinning gyroscopes, and not interfere with the operation of the SQUID readout system. Considerable improvement in the sensitivity of the gyroscopes or proof masses as differential accelerometers could be achieved for a system that was specifically designed for that purpose. The specific force noise on the unsupported gyroscope is expected to be considerable smaller, but there is no convenient method of measuring this specific force noise on the satellite.

ACKNOWLEDGEMENTS

The authors would like to thank Stephano Vitale for valuable discussions.

REFERENCES

1. J. P. Turneaure, C. W. F. Everitt, B. W. Parkinson *et al.*, Adv. Space Res. (UK) **9**, 29-38 (1989).
2. W de Sitter, Mon. Not. Royal Astr. Soc. **77**, 155-184 (1916).
3. J. Lense and H. Thirring, Phys. Z. **19**, 156 (1918).
4. B. Mashhoon, F. W. Hehl, and D. S. Theiss, General Relativity and Gravitation **16**, 711-750 (1984).
5. Y. R. Jafry, *Aeronomy Coexperiments on Drag-Free Satellites with Proportional Thrusters: GP-B and STEP*, Ph. D. Thesis, Stanford University, 1992.
6. M. B. Tapley, *A Geodetic Gravitation Gradiometer Coexperiment to Gravity Probe B* , Ph. D. Thesis, Stanford University, 1993.
7. M. Tapley, J. Breakwell, C.W.F. Everitt *et al.*, Adv. in Space Res. **11**, 179-82 (1991).
8. S. Buchman, T. Quinn, G. M. Keiser *et al.*, Rev. Sci. Instr. **66**, 120-9 (1995).
9. W. R. Smythe, *Static and Dynamic Electricity*, New York: Hemisphere Publishing Corp, 1989, pp. 39-40.
10. G. F. Franklin and J. D. Powell, *Digital Control of Dynamic Systems,* Reading, Mass.: Addison-Wesley, 1981.
11. C. C. Speake, Classical and Quantum Gravity **13**, A291-A297 (1996).
12. P. Zhou, S. Buchman, K. Davis *et al.*, Surface and Coatings Technology **77**, 516-20 (1995).
13. N. J. Kasdin and C. Gauthier, J. Astronautical Sciences 44, 129-147 (1996).
14. R. Whelan, Lockheed-Martin Engineering Memorandum Report No. GPB-10742, 1996.
15. J. Kirshcenbaum, Lockheed-Martin Engineering Memorandum Report No. ATCS 210, 1995.